Block of T cell development in P53-deficient mice accelerates development of lymphomas with characteristic RAG-dependent cytogenetic alterations

Brian B. Haines,[1,7] Chun Jeih Ryu,[1,2,7] Sandy Chang,[3,6] Alexei Protopopov,[3] Andreas Luch,[1] Yun Hee Kang,[2,5] Dobrin D. Draganov,[1] Maria F. Fragoso,[1] Sang Gi Paik,[5] Hyo Jeong Hong,[2] Ronald A. DePinho,[3,4] and Jianzhu Chen[1,*]

[1] Center for Cancer Research and Department of Biology, Massachusetts Institute of Technology, Cambridge, Massachusetts 02139
[2] Laboratory of Antibody Engineering, Korea Research Institute of Bioscience and Biotechnology, Yusong, Daejon 305-600, Korea
[3] Department of Medical Oncology, Dana-Farber Cancer Institute, Boston, Massachusetts 02115
[4] Departments of Medicine and Genetics, Harvard Medical School, Boston, Massachusetts 02115
[5] Department of Biology, Chungnam National University, Daejon 305-600, Korea
[6] Department of Molecular Genetics, M.D. Anderson Cancer Center, Houston, Texas 77030
[7] These authors contributed equally to this work.
*Correspondence: jchen@mit.edu

Summary

Mice deficient in the DNA damage sensor P53 display normal T cell development but eventually succumb to thymic lymphomas. Here, we show that inactivation of the TCR β gene enhancer (Eβ) results in a block of T cell development at stages where recombination-activating genes (RAG) are expressed. Introduction of the Eβ mutation into *p53*$^{-/-}$ mice dramatically accelerates the onset of lethal thymic lymphomas that harbor RAG-dependent aberrant rearrangements, chromosome 14 and 12 translocations, and amplification of the chromosomal region 9A1–A5.3. Phenotypic and genetic analyses suggest that lymphomas emerge through a normal thymocyte development pathway. These findings provide genetic evidence that block of lymphocyte development at stages with RAG endonuclease activity can provoke lymphomagenesis on a background with deficient DNA damage responses.

Introduction

DNA double-strand breaks (DSBs), generated by both physiological processes and physicochemical damages, represent a serious breach of genome integrity that can trigger the onset of cell cycle arrest, apoptosis, or tumorigenesis (Khanna and Jackson, 2001; van Gent et al., 2001). Normally, DSBs are efficiently repaired by nonhomologous end joining (NHEJ) during the G_0/G_1 phase or homologous recombination during the S/G_2 phase. V(D)J recombination is a programmed DNA cleavage and repair process by which T cell receptor (TCR) and immunoglobulin (Ig) genes are assembled from spatially dispersed gene segments (Fugmann et al., 2000). Recombination is initiated when the lymphocyte-specific proteins RAG1 and RAG2 (referred to as RAG) cut DNA at the junction of coding sequences and recombination signal sequences (RSS) (McBlane et al., 1995), producing covalently sealed coding ends and blunt signal ends (Roth et al., 1992; Schlissel et al., 1993). The resulting DSBs are then repaired by NHEJ, involving the DNA-dependent protein kinase (Ku70/Ku80/DNA-PKcs), Artemis, and the Xrcc4/ligase IV complex (Chu, 1997). V(D)J recombination has served as a model for the study of physiological DNA rearrangement and repair in vertebrates and the effect of persistent DSBs on chromosomal translocations and tumorigenesis (Bassing et al., 2002).

Assembly and expression of antigen receptor genes is critical for lymphocyte development and survival. For T cells expressing the αβ TCR, development progresses from $CD4^-CD8^-$ (double negative [DN]) thymocytes to $CD4^+CD8^+$ (double positive [DP]) thymocytes and finally to mature $CD4^+$ or $CD8^+$ (single positive [SP]) T cells (Rothenberg and Taghon, 2005). Depending on the status of CD44 and CD25 expression, DN thymocytes are further divided into four successive subpopulations: $CD44^+CD25^-$ (DN1), $CD44^+CD25^+$ (DN2), $CD44^-CD25^+$ (DN3), and $CD44^-CD25^-$ (DN4). RAG is first expressed in DN3

SIGNIFICANCE

DNA recombination and repair pathways are central to the development of normal cells, and aberrations in these pathways have been linked to cancer. The programmed DNA cleavage mediated by the RAG endonuclease during lymphocyte development has served as a model for the study of the effect of persistent DNA breaks on chromosomal translocations and tumorigenesis. We show that block of T cell development at stages where RAG genes are expressed accelerates development of thymic lymphomas in mice with deficient DNA damage responses. The lymphomas harbor RAG-dependent chromosome translocations and amplifications frequently associated with human hematological malignancies. Thus, lymphocyte developmental arrest and the associated persistent RAG activity represent a heretofore underappreciated but potentially important factor in lymphomagenesis.

thymocytes to rearrange *TCRβ* (Dudley et al., 1994; Godfrey et al., 1994). Functional assembly of *TCRβ* leads to expression of the pre-TCR complex, which consists of TCRβ, pTα, and CD3 proteins and signals proliferation and differentiation of DN thymocytes and cessation of RAG expression (Levelt and Eichmann, 1995). In DP thymocytes, RAG is reexpressed to rearrange *TCRα*. Functional assembly of *TCRα* leads to expression of the complete TCR, consisting of TCRβ, TCRα, and CD3 proteins, which signals the development of SP T cells and permanent inactivation of RAG expression. Accordingly, failure to express pre-TCR or TCR leads to a block of thymocyte development at the DN3 or DP stage, respectively, at which RAG is naturally expressed. Thymocytes that fail to produce a functional TCRβ protein are eliminated by apoptosis via a mechanism that may involve the tumor suppressor protein P53 (Haks et al., 1999).

Normally, RAG-mediated cleavages during V(D)J recombination are tightly coupled to the efficient NHEJ repair pathway (Lee et al., 2004) in that coding ends are rapidly and efficiently opened, modified, and joined, minimizing the chance of aberrant joining and chromosomal translocations. Attesting to the efficiency of NHEJ repair, P53 is not activated by DSBs generated during V(D)J recombination in wild-type mice (Guidos et al., 1996). In cases of persistent DSBs brought about by defects during V(D)J recombination, mechanisms exist to either sense and repair the breaks or eliminate cells with persistent DSBs. P53 is critical for such cellular responses to DNA damage (Khanna and Jackson, 2001; van Gent et al., 2001). For example, P53 is activated in developing thymocytes in mice deficient in DNA-PKcs because DSBs generated during V(D)J recombination cannot be repaired by NHEJ (Guidos et al., 1996; Haks et al., 1999). Because of P53-mediated cell cycle arrest and apoptosis, only a small percentage of NHEJ mutant mice develop T cell lymphoma, and then only after a latency period of 6 months or more (Difilippantonio et al., 2000; Gu et al., 1997; Jhappan et al., 1997; Li et al., 1998).

Nevertheless, defective V(D)J recombination has been linked to chromosomal translocations and tumorigenesis (Tycko and Sklar, 1990; Vanasse et al., 1999). The most convincing and detailed studies have utilized mutant mice that are defective in the repair of RAG-mediated DSBs, as a result of deletion of a component of NHEJ machinery, and cellular responses to persistent DSBs, as a result of loss of P53 function (Bassing et al., 2002). P53-deficient mice display grossly normal T cell development and repertoire but succumb to thymic lymphomas by 6 months of age, independent of RAG-mediated V(D)J recombination (Nacht et al., 1996). However, $p53^{-/-}$ *NHEJ*$^{-}$ mutant mice rapidly develop lethal pro-B cell lymphomas by 10 weeks of age (Difilippantonio et al., 2000, 2002; Frank et al., 2000; Gao et al., 2000; Nacht et al., 1996). Most importantly, pro-B cell lymphomas harbor RAG-dependent translocations between the *IgH* and c-*myc* through a complex breakage-fusion-bridge (B-F-B) process (Gladdy et al., 2003; Zhu et al., 2002). These findings show that, in the absence of P53 and NHEJ repair, RAG-induced DSBs promote rapid development of B cell lymphomas. However, given the multiple roles NHEJ factors play in general genome integrity, DSB repair, and V(D)J recombination, precise assessment of RAG activity in lymphomagenesis in these NHEJ mutant models is challenging.

Here, we report the impact of RAG activity on lymphomagenesis in the presence of an intact NHEJ pathway in mice. This study takes advantage of P53-deficient mice whose TCR β gene enhancer (Eβ) is inactivated. In the absence of the Eβ, *TCRβ* rearrangement and transcription are blocked, leading to arrest of T cell development at the DN stage (Bouvier et al., 1996; Ryu et al., 2003), where *RAG* is naturally expressed. We show that (1) Eβ mutation dramatically accelerates the onset of lethal thymic lymphoma in $p53^{-/-}$ mice; (2) the T cell lymphomas exhibit RAG-dependent chromosome 12 and 14 translocations and amplification of the chromosomal region 9A1–A5.3; and (3) progression of lymphomagenesis goes through the normal thymocyte development pathway. The unique experimental attributes of the Eβ mutation provide an opportunity to assess the cytogenetic and carcinogenic consequences of expression of endogenous *RAG* that are confined to the physiologically relevant stages of thymocyte development. Our results raise the fundamental possibility that any genetic aberration leading to an early lymphocyte block and persistent *RAG* expression can act as a procarcinogenic event.

Results

Thymocytes express RAG2 and undergo massive apoptosis in $E\beta^{R/R}$ mice

The Eβ is a major *cis* element known to regulate *TCRβ* rearrangement and transcription. Its inactivation, either by deletion or replacement with Gal4 DNA sequences (referred to as $E\beta^{-/-}$ and $E\beta^{R/R}$, respectively), in mice results in a severe block of Dβ to Jβ rearrangement and collapse in thymocyte cellularity (Bouvier et al., 1996; Mathieu et al., 2000; Ryu et al., 2003). Thymocyte development in $E\beta^{R/R}$ mice is primarily blocked at the DN stage (Figure 1A). A significant number of cells progress to the DP stage, presumably due to selection via TCRγδ because $E\beta^{R/R}$ $TCR\delta^{-/-}$ (referred to as ED) mice display a completely DN block (Figure 1A). As expected, DN thymocytes of αβ lineage in $E\beta^{R/R}$ and ED mice were arrested at the $CD44^{-}CD25^{+}$ (DN3) stage (Figure 1A, lower panel), when *TCRβ* rearrangement normally occurs. These findings in $E\beta^{R/R}$ mice are identical to those observed in the $E\beta^{-/-}$ mice (Leduc et al., 2000).

To verify the expression of RAG in DN and DP thymocytes of $E\beta^{R/R}$ mice, we used mice in which a *RAG2-GFP* fusion gene was knocked into the endogenous *RAG2* locus (Monroe et al., 1999). As shown in Figure 1B, most αβ lineage thymocytes from $RAG2^{+/GFP}$ mice were RAG2 positive, as indicated by GFP expression. Compared to those of $RAG2^{+/GFP}$ mice, DN and/or DP thymocytes from $E\beta^{R/R}$ $RAG2^{+/GFP}$ and ED $RAG2^{+/GFP}$ mice expressed equivalent levels of RAG2.

To examine the fate of $E\beta^{R/R}$ thymocytes, DN and DP thymocytes from 4- to 6-week-old mice were assayed for apoptosis by staining with annexin V. Approximately 60% of DN and 80% of DP thymocytes of $E\beta^{R/R}$ mice were apoptotic, representing approximately 9- and 18-fold increases, respectively, over wild-type counterparts (5%–7%) (Figure 1C). To investigate the role of P53 in the apoptosis of the $E\beta^{R/R}$ thymocytes, we generated $E\beta^{R/R}$ $p53^{-/-}$ mice (referred to as EP mice). The percentages of apoptotic EP thymocytes were about 24% (DN) and 36% (DP), representing a reduction of approximately 2-fold relative to those of $E\beta^{R/R}$ thymocytes (Figure 1C). Nevertheless, the proportions of apoptotic thymocytes in EP mice were still significantly higher than those in wild-type or $p53^{-/-}$ mice. Together, these results show that most $E\beta^{R/R}$ thymocytes express RAG2

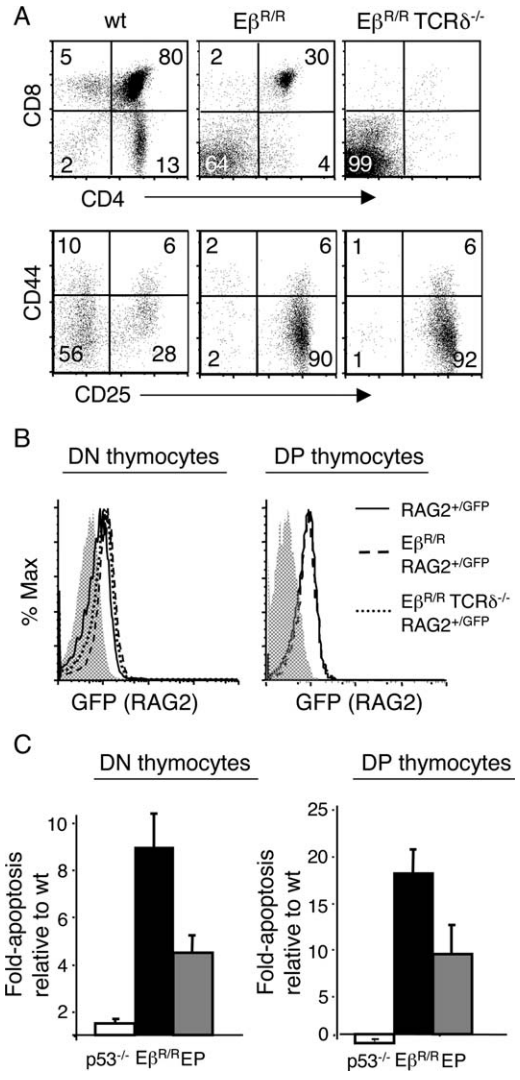

Figure 1. Thymocyte development, RAG2 expression, and apoptosis in $E\beta^{R/R}$ mice

A: Comparison of thymocyte phenotypes of wild-type (wt), $E\beta^{R/R}$, and $E\beta^{R/R}$ $TCR\delta^{-/-}$ mice. Thymocytes were stained with antibodies specific for CD4, CD8, TCRγδ, CD44, and CD25. CD4 versus CD8 staining profiles are shown for total thymocytes (top row). CD44 versus CD25 staining profiles are shown for TCRγδ-negative DN thymocytes (lower row).

B: RAG2 expression in DN and DP thymocytes. One copy of GFP-tagged RAG2 was bred into wt, $E\beta^{R/R}$, and $E\beta^{R/R}$ $TCR\delta^{-/-}$ mice. Thymocytes without GFP-tagged RAG2 were used as a negative control (shaded areas). TCRγδ thymocytes were excluded from analysis.

C: Effect of the $E\beta^{R/R}$ mutation on thymocyte apoptosis. Thymocytes from 4- to 6-week-old wt, $p53^{-/-}$, $E\beta^{R/R}$, and EP mice were stained for CD4, CD8, TCRγδ, annexin V, and DAPI. Percentages of annexin$^+$ DAPI$^-$ apoptotic cells were quantified for TCRγδ-negative DN and DP thymocytes. Shown are fold changes in the percentage of apoptotic cells in indicated mice relative to wt mice. Data are from three independent experiments with at least two mice per genotype per experiment. Error bars indicate the standard deviation of percentage apoptotic cells within each genotype set.

and undergo massive apoptosis by mechanisms that partly involve P53.

The $E\beta^{R/R}$ mutation accelerates the development of thymic lymphoma in $p53^{-/-}$ mice

The $E\beta^{R/R}$ mouse model provides a direct means of assessing the lymphomagenic potential of RAG expression in the setting of normal DNA DSB repair. As shown in Figure 2A, all $E\beta^{+/R}$ and $E\beta^{R/R}$ mice remained free of thymic neoplasm over a 12 month observation period. Consistent with previous reports (Jacks et al., 1994; Nacht et al., 1996), approximately 70% of $p53^{-/-}$ mice succumbed to thymic lymphomas with a mean survival of ~22 weeks. In contrast, 12 of 18 EP mice developed thymic lymphoma with a mean survival of 14 weeks (Figure 2A), as determined by necropsy, histology (Figure 2B), and flow cytometry (Figures 2C and 2D). Lymphomas arising in EP mice mostly remain in the thymus and only inefficiently spread to other organs, presumably due to the absence of TCR (Engel and Murre, 2002). The accelerated onset of lethal thymic lymphomas in EP mice was not a result of differences in genetic background because both strains were on similar C57BL/6 backgrounds and EP mice derived from different mating strategies exhibited similarly uniform and rapid disease progression. Thus, lymphomagenesis is accelerated in $p53^{-/-}$ mice in the absence of the Eβ.

Progression of lymphomagenesis through DP stage in $E\beta^{R/R}$ $p53^{-/-}$ mice

Freshly isolated lymphoma cells from different EP mice expressed high levels of Thy-1, CD8, variable levels of CD4, but not B220 (Figure 2D and data not shown), confirming their T cell identity. Unlike mature CD8 SP thymocytes from wild-type or $p53^{-/-}$ mice, CD8-positive lymphoblasts from EP mice expressed high levels of CD24 but very low levels of CD5, CD69, IL-7Rα, and Qa2 (Figure 2C and data not shown), indicating an immature developmental stage and a lack of proper positive selection (Bendelac et al., 1992). In support of this interpretation, CD8$^+$ thymocytes in EP mice did not express TCRβ on the cell surface or within the cell (data not shown).

We next examined the onset and progression of lymphoma development in EP mice. Through 5–6 weeks of age, EP mice had identical proportions of DN and DP thymocytes as $E\beta^{R/R}$ mice (Figure 2D). By 7 weeks of age, however, some DP thymocytes started to lose CD4 expression and gradually became CD8 SP. A significant fraction of DP and SP cells were large and actively cycling, and some were aneuploid (Figure 2D). By 8 weeks of age, over 60% of the thymocytes were CD8 SP. By 11–17 weeks, mice developed terminal thymic lymphomas characterized by massive expansion of large, aneuploid CD8 SP cells and sometimes DP cells (Figure 2D), which were readily propagated in vitro.

A characteristic feature of lymphoma development in EP mice is an initial increase in the proportion of DP thymocytes followed by the appearance of DP and CD8 SP tumor cells. To investigate the requirement for TCRγδ-mediated DP thymocyte development in lymphomagenesis, we generated $E\beta^{R/R}$ $p53^{-/-}$ $TCR\delta^{-/-}$ (referred to as EPD) mice. Before 4 weeks of age, almost all thymocytes in EPD mice were DN (Figure S1 in the Supplemental Data available with this article online), similar to ED mice. As mice aged, however, DP thymocytes first appeared, followed by CD8 SP cells. Freshly isolated lymphoma cells from terminally ill EPD mice were DP or CD8 SP, cycling, and aneuploid (Figure S1). Similar to EP mice, the mean survival of EPD mice was 14 weeks. These results suggest that lymphoma development in EP and EPD mice is very similar both in terms of kinetics and the phenotype of the emergent lymphoma cells. They further suggest that lymphomas develop from the DN precursors of αβ lineage thymocytes and that progression to the DP

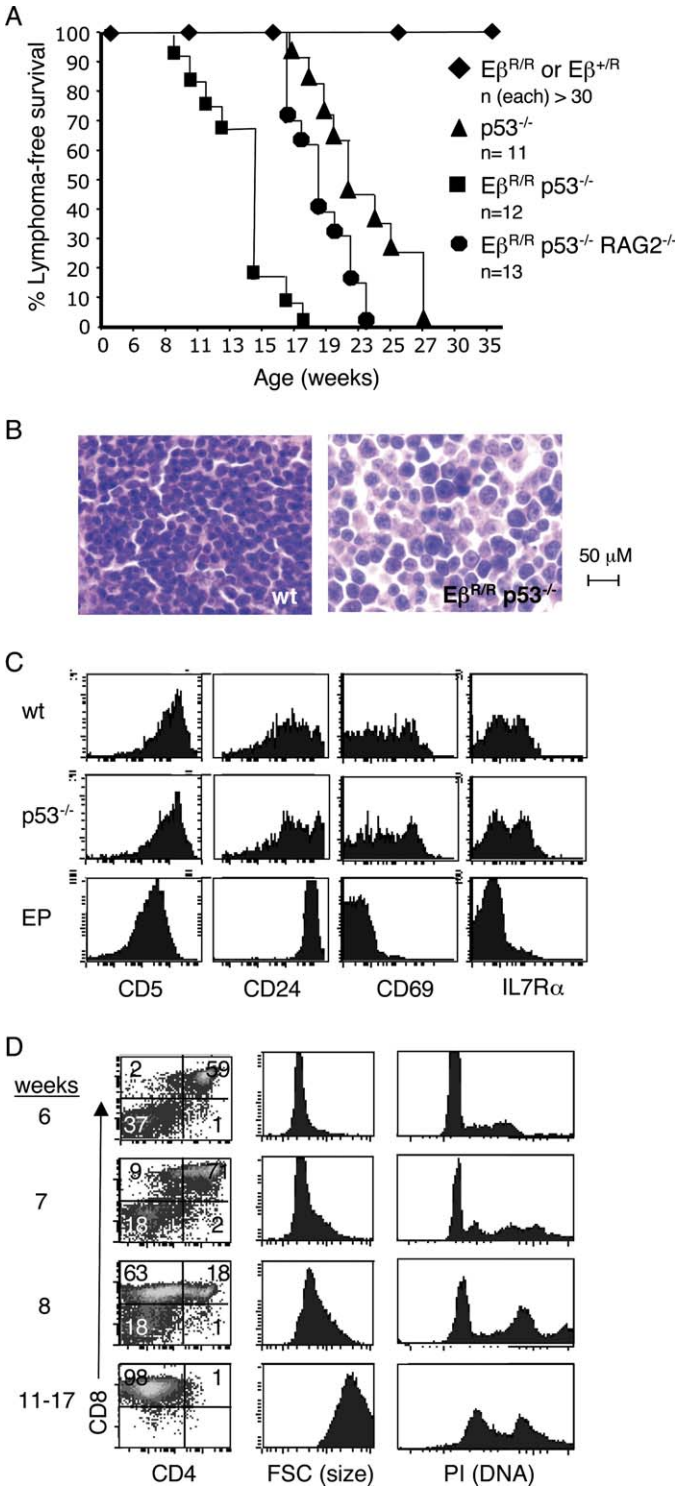

Figure 2. *Eβ*$^{R/R}$ mutation synergizes with P53 deficiency in development of thymic lymphomas

A: Survival of a cohort of *Eβ*$^{R/R}$, *p53*$^{-/-}$, *Eβ*$^{R/R}$ *p53*$^{-/-}$, and *Eβ*$^{R/R}$ *p53*$^{-/-}$ *RAG2*$^{-/-}$ mice was followed over the indicated time period. Numbers of mice (n) in each group are indicated. A subset of mice, including 6 out of 18 EP mice, 5 out of 18 EPR mice, and 4 out of 15 *p53*$^{-/-}$ mice, died between 3 and 7 weeks of age due to causes other than thymic lymphoma and were therefore excluded from the survival plot.

B: Hemoxylin and eosin stain of thymus sections of a wt and a terminally ill *Eβ*$^{R/R}$ *p53*$^{-/-}$ mouse (14 weeks). Magnification 40×. Note that thymic cytoarchitecture of EP mice is replaced with monotonous fields of large, highly mitotic lymphoblasts.

C: Comparison of surface phenotype of CD8 SP thymocytes among wt, *p53*$^{-/-}$, and EP mice. Thymocytes of 6- to 8-week-old mice were stained for CD4, CD8, and TCRγδ, as well as CD5, CD24, CD69, or IL-7Rα. Shown is expression of various markers for TCRγδ^{-} CD8 SP thymocytes.

D: Progression of lymphomagenesis in *Eβ*$^{R/R}$ *p53*$^{-/-}$ mice. Thymocytes from EP mice at indicated ages were stained for CD4, CD8, TCRγδ, and propidium iodide (PI). Left panel: CD4 versus CD8 staining profiles of TCRγδ^{-} thymocytes (PI^{-}); percentages of cells in each quadrant are shown. Middle panel: cell size (FSC, forward scatter) of TCRγδ^{-} DP and CD8 SP cells. Right panel: DNA content of TCRγδ^{-} DP and CD8 SP cells. Most of the thymocytes (>95%) in *Eβ*$^{R/R}$ mice at the indicated ages were either DN or DP as shown in Figure 1A.

stage, by a mechanism independent of TCRγδ, is associated with lymphomagenesis.

RAG2 is expressed during the course of lymphomagenesis and in resulting lymphoma lines

Based on the effect of the *Eβ* mutation on T cell development as well as the critical role of P53 in mediating cellular responses to DSBs, we investigated the role of RAG activity in lymphomagenesis in EP mice. To begin to test this mechanism, we followed *RAG2* expression during the course of lymphomagenesis by introducing the GFP-tagged RAG2 allele into EPD mice or their littermates (*Eβ*$^{R/R}$ *p53*$^{+/-}$ *TCRδ*$^{-/-}$). As with EP or EPD mice, development of thymic lymphomas in EPD *RAG2*$^{+/GFP}$ mice exhibited a similar kinetics and phenotypic progression. Thus, at 4 weeks of age, thymocytes from EPD *RAG2*$^{+/GFP}$ mice were all DN (Figure 3A). By 8 weeks of age, DP and CD8 SP lymphoblasts appeared, and by 14 weeks of age, most thymocytes were DP or CD8 SP in terminally ill mice (Figure 3A). Importantly, DP thymocytes from EPD *RAG2*$^{+/GFP}$ mice at both the intermediate (8 week) and terminal stage (14 week) expressed RAG2 (Figure 3B). Similarly, RAG2 expression was detected in DP cells during lymphomagenesis in EP mice and in lymphoma cells that had been cultured for 2 weeks (data not shown). In addition, *RAG2* transcripts were readily detected by Northern blotting in all three randomly selected EP lymphoma lines that had been cultured for months, whereas no expression was detected in a *p53*$^{-/-}$ lymphoma line (Figure 3C). Together, these results suggest that RAG is expressed during lymphomagenesis and in resulting lymphoma cells, supporting the possibility that RAG-induced aberrant cleavages may have contributed to the accelerated lymphoma development in EP mice.

Both normal and aberrant RAG-mediated rearrangements occur in *Eβ*$^{R/R}$ *p53*$^{-/-}$ lymphomas

Next, we examined RAG activity by assaying for the presence of rearrangements at antigen receptor loci and other genomic loci in EP lymphomas. Genomic DNA from both *p53*$^{-/-}$ and EP lymphomas and from thymocytes of wild-type and mutant mice was analyzed by Southern blotting. Hybridization with probes from Dβ1–Jβ1, Dβ2–Jβ2, and Cβ1 regions (Figure 4A) revealed that the Dβ1–Jβ1 region and to a lesser extent the Dβ2–Jβ2 region were rearranged in wild-type thymocytes but not in *Eβ*$^{R/R}$, EP, and *RAG2*$^{-/-}$ thymocytes (Figures 4B–4D). Similarly, the Dβ1–Jβ1 region was rearranged in two of the three *p53*$^{-/-}$ lymphoma lines, consistent with normal T cell development in *p53*$^{-/-}$ mice. In contrast, both Dβ1–Jβ1 and Dβ2–Jβ2 regions were in germline configuration in all seven EP lymphoma lines (Figures 4B–4D). These results were further confirmed by PCR amplification

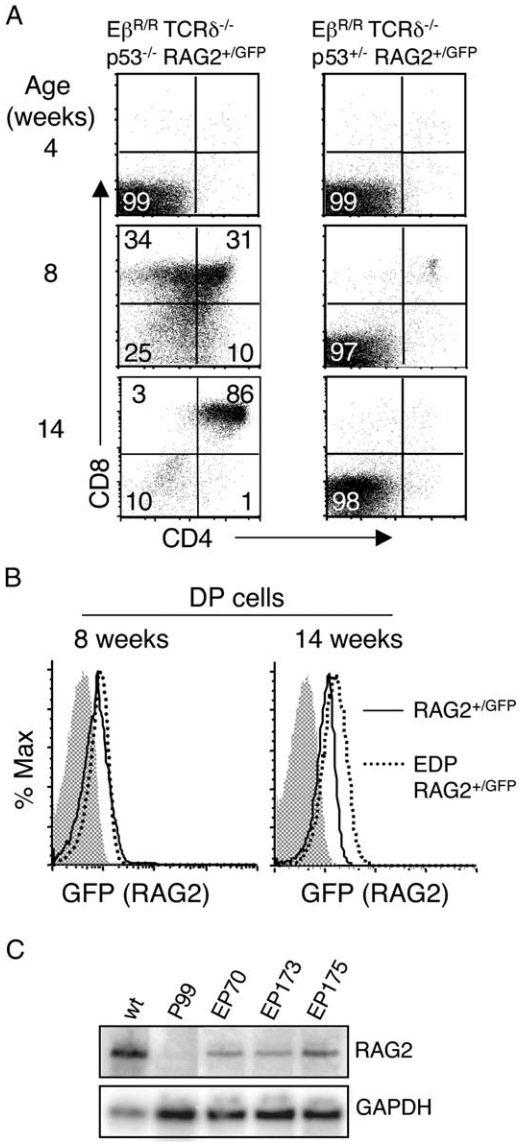

Figure 3. RAG2 is expressed during the course of lymphomagenesis and in lymphoma lines

A and B: Tracking RAG2 expression during lymphomagenesis. GFP-tagged RAG2 was introduced into EPD mice and littermate controls (with one wild-type p53 allele). At indicated ages, thymocytes were assayed for CD4, CD8, and GFP (RAG2) expression. CD4 versus CD8 staining profiles are shown for total thymocytes (**A**), and GFP (RAG2) expression is shown for DP thymocytes of 8-week-old and terminal 14-week-old mice (**B**). DP thymocytes from wild-type mice were used as a negative control (shaded areas).

C: Northern blotting analysis of RAG2 transcripts in total RNA from a $p53^{-/-}$ (P99) and EP (EP70, EP173, and EP175) thymic lymphoma lines. RNA from wild-type thymus is included as a positive control. Hybridization with a GAPDH probe is used to normalize the relative level of RNA loading in different lanes.

and sequencing of the DNA regions containing Dβ1, Jβ1.4, and Jβ1.5 gene segments in the seven lymphomas (data not shown). Thus, the gross translocation of the *TCRβ* locus is not a contributing factor to the observed acceleration of lymphoma development in EP mice.

The same blot was hybridized with a Jα49-48 probe from the 5′ end of the Jα region of the *TCRα* locus. As expected,

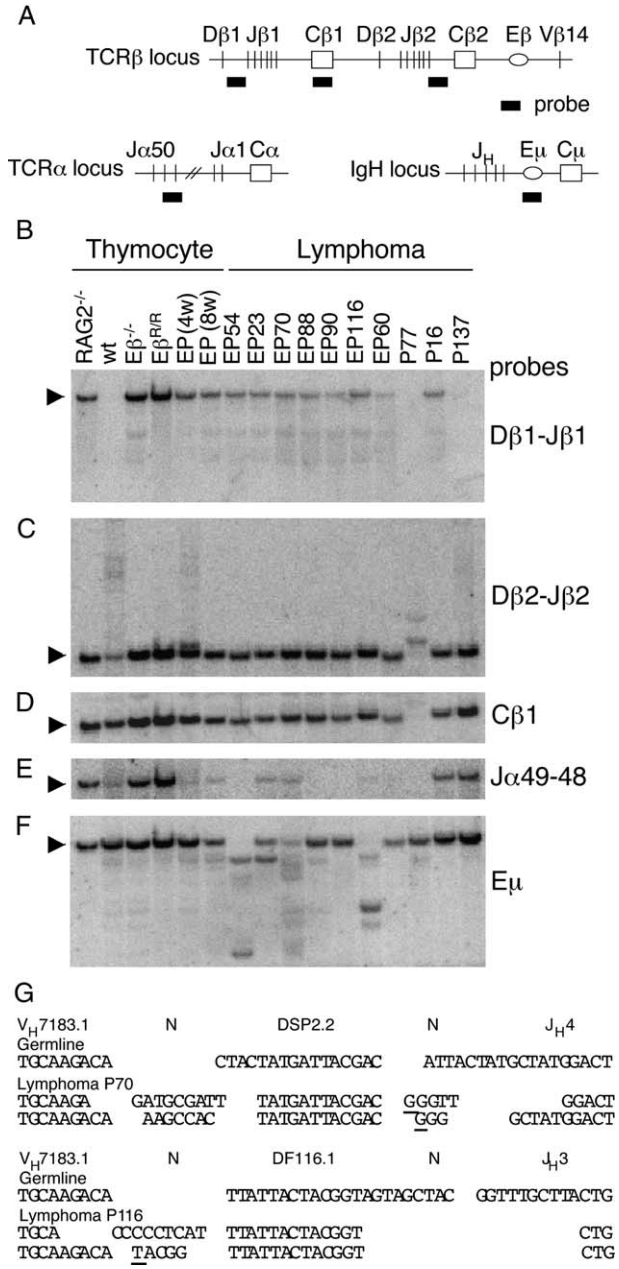

Figure 4. RAG-mediated rearrangements at the *TCRα* and *IgH* loci in $Eβ^{R/R}$ $p53^{-/-}$ lymphomas

A: Schematic diagrams of the *TCRβ*, *TCRα*, and *IgH* loci and the position of probes used.

B–F: Southern blotting analyses of rearrangements at the *TCRβ*, *TCRα*, and *IgH* loci in thymocytes and thymic lymphomas. Genomic DNA was digested with EcoR1, separated on an agarose gel, transferred to a filter, and hybridized with various probes successively (from top to bottom) after removal of the previous probe. Thymic lymphomas from EP mice are labeled as EP54, etc., and those from $p53^{-/-}$ mice are labeled as P77, etc. The rest of the DNA samples were from thymocytes of indicated mice. Two EP mice, one at 4 weeks of age and the other at 8 weeks of age, were used. Arrows indicate germline fragments.

G: Sequences of *IgH* rearrangements from thymic lymphomas EP70 and EP116. *IgH* rearrangements were amplified by digestion-circularization PCR and then cloned and sequenced. Specific gene segments used in rearrangements are identified. N nucleotides are indicated, and possible P nucleotides are underlined.

a germline fragment was detected in thymocyte DNA from *RAG2*$^{-/-}$ mice (Figure 4E). In contrast, the Jα49-48-hybridizing signal was greatly reduced in thymocyte DNA from wild-type mice, indicating deletion of the Jα region by rearrangement. The Jα49-48-hybridizing signal was also absent or greatly reduced in all EP lymphomas and the three *p53*$^{-/-}$ lymphomas, indicating *TCRα* rearrangements. Notably, the Jα49-48-hybridizing signal was abundant in thymocyte DNA from both *Eβ*$^{-/-}$ and *Eβ*$^{R/R}$ mice but greatly diminished in that from both 4- and 8-week-old EP mice. The lack of *TCRα* rearrangements in *Eβ*$^{R/R}$ mice could reflect the rapid apoptosis of these cells whereas EP thymocytes have a prolonged survival and an opportunity to undergo RAG-mediated rearrangements.

To investigate the presence of RAG-mediated aberrant rearrangements in EP lymphomas, we assayed for *IgH* J_H rearrangements using a probe spanning the intronic enhancer (Eμ; Figure 4A). As expected, the J_H region was in germline configuration in wild-type, *RAG2*$^{-/-}$, *Eβ*$^{R/R}$, and EP thymocytes, and in *p53*$^{-/-}$ thymic lymphomas. In contrast, four of the seven EP lymphoma lines had undergone J_H rearrangements, as indicated by the presence of at least one nongermline J_H fragment (Figure 4F). In two of the four EP lymphoma lines (EP54 and EP116), the germline J_H fragment was completely absent, indicating a complete J_H rearrangement on both alleles. Cloning and sequencing of some of these Eμ-hybridizing nongermline fragments from lymphomas EP70 and EP116 revealed that all four independent clones were derived from complete V_H-D-J_H rearrangements (Figure 4G). In particular, the two V_H-D-J_H rearrangements from lymphoma EP116 had identical D-J_H junctional sequences but different V_H to DJ_H rearrangements. Given that the complete V_H-D-J_H rearrangements are extremely rare in T cells in wild-type mice, these results support the view that RAG expression in EP thymocytes can result in aberrant rearrangements.

Further evidence for RAG-mediated aberrant rearrangements in EP lymphomas was obtained by assaying for internal deletion at the *Bcl11b* locus, which contains cryptic RSS and is accessible to RAG in DN thymocytes (Sakata et al., 2004). PCR products of approximately the correct size were detected in all six EP lymphoma lines but not in two *p53*$^{-/-}$ lymphoma lines (Figure 5B). The PCR products were also absent in three lymphoma lines from *Eβ*$^{R/R}$ *p53*$^{-/-}$ *RAG2*$^{-/-}$ (referred to as EPR) mice, indicating a requirement of RAG2 for the internal deletion. Furthermore, sequences of PCR products from all seven EP lymphoma lines displayed hallmarks of RAG-mediated rearrangements at the joints, including nucleotide deletions, nontemplated nucleotide additions (N), and palindromic (P) sequences. However, by Southern blotting, a large proportion of *Bcl11b* locus remained in the germline configuration in EP lymphomas (data not shown), suggesting that *Bcl11b* deletions are secondary to lymphomagenesis and reflect ongoing RAG activity in lymphoma lines. Taken together, these results strongly suggest that RAG can aberrantly cleave both antigen receptor loci that are normally inaccessible in T cells and nonantigen receptor loci in EP lymphomas.

Eβ$^{R/R}$ *p53*$^{-/-}$ lymphomas exhibit RAG-dependent recurrent chromosomal alterations

We next examined chromosomal alterations in EP lymphomas by spectral karyotyping (SKY). As shown in Figure 6 and Table 1, *p53*$^{-/-}$ lymphomas displayed extensive numerical

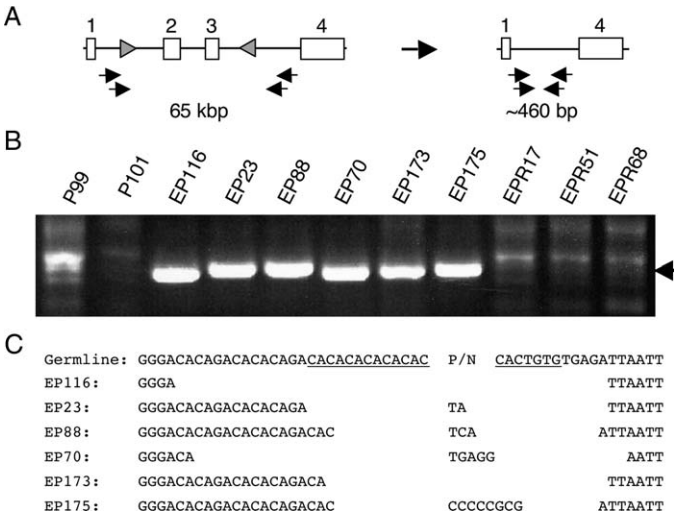

Figure 5. RAG-mediated internal deletion at the *Bcl11b* locus in *Eβ*$^{R/R}$ *p53*$^{-/-}$ lymphomas

A: Schematic diagrams of the PCR assay for *Bcl11b* internal deletion. PCR amplification of *Bcl11b* is only possible upon internal deletion of exons 2 and 3 as the primers are 65 kb apart. Open boxes, exons; gray triangles, cryptic RSS; and arrows, PCR primers.

B: Ethidium bromide staining of PCR products amplified from independently derived *p53*$^{-/-}$, *Eβ*$^{R/R}$ *p53*$^{-/-}$, and *Eβ*$^{R/R}$ *p53*$^{-/-}$ *RAG2*$^{-/-}$ lymphoma lines. Arrow indicates the correct product.

C: Junctional sequences of *Bcl11b* internal deletion products. PCR products from B were cloned and sequenced and compared to germline sequences. Nucleotide deletions and P and N nucleotides are indicated. Cryptic RAG recognition sites in the germline *Bcl11b* locus are underlined.

chromosomal aberrations, with infrequent nonclonal translocations, as previously reported (Difilippantonio et al., 2002; Liao et al., 1998). While EP lymphomas resembled *p53*$^{-/-}$ lymphomas (exhibiting extensive numerical chromosomal aberrations), distinct karyotypic events were evident, including frequent translocations involving chromosomes 9, 12, or 14. Among 52 translocations detected in 69 spreads, 47 translocations involved chromosomes 9, 12, or 14, a frequency significantly higher than expected from a random event ($p < 0.0001$). Similarly, EPD lymphomas harbored frequent chromosome 9 translocations (12 out of 16 in 26 spreads). Chromosomes 12 and 14 harbor the *IgH* and *TCRα* loci, respectively, raising the possibility that these translocations are initiated by RAG-mediated cleavages at those loci. Consistent with this possibility, lymphomas from EPR mice that were deficient in *RAG2* had no chromosome 9, 12, or 14 translocations among 32 metaphase spreads examined in three independent lymphoma lines. Even among 46 spreads examined in five *p53*$^{-/-}$ lymphoma lines, only 5 of 28 translocations involved chromosomes 9, 12, or 14, a frequency not significantly different from that expected from a random event ($p = 0.23$). Compared to those in EPR or *p53*$^{-/-}$ lymphomas, the frequency of chromosome 9, 12, or 14 translocations was significantly higher in EP lymphomas ($p < 0.0001$ for both comparisons). There was no statistical difference in the frequency of chromosome 9, 12, or 14 translocations between EPR and *p53*$^{-/-}$ lymphomas ($p = 0.31$). Together, these results suggest that RAG activity is required for the generation of chromosomal aberrations characteristic of EP lymphomas.

To examine genomic aberrations in EP lymphomas in greater detail, we performed array-based comparative genomic

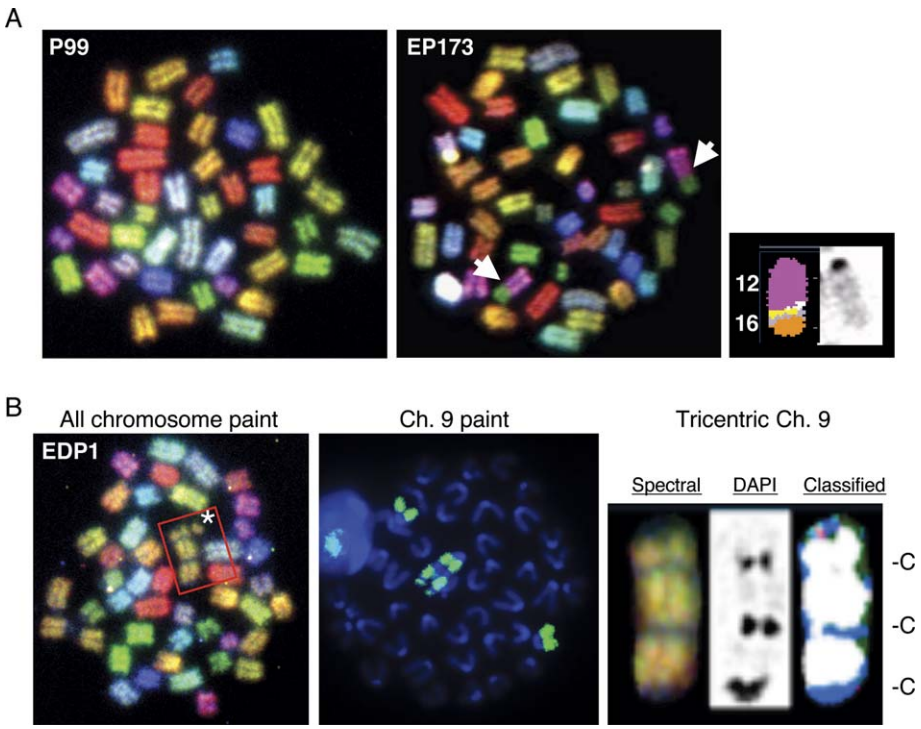

Figure 6. Spectral karyotype analysis of $E\beta^{R/R}$ $p53^{-/-}$ lymphomas

A: Examples of spectral images of thymic lymphomas from $p53^{-/-}$ (P99, left panel) and $E\beta^{R/R}$ $p53^{-/-}$ (EP173, right panel) mice. The white arrows indicate two t(12;16) translocations observed in a EP173 metaphase spread. The right panel shows the classified (left) and DAPI (right) images of one of the t(12;16) translocations.

B: SKY analyses of an $E\beta^{R/R}$ $p53^{-/-}$ $TCR\delta^{-/-}$ lymphoma (EDP1). Spectral all-chromosome paint (left panel) and chromosome 9-specific paint (middle panel) images are shown. Tricentric chromosome 9 is boxed, and asterisk indicates a chromosome 9 fragment. In the right panel, spectral, DAPI, and classified images of the tricentric chromosome 9 are indicated. C indicates centromere, which does not stain.

hybridization (array CGH) analyses on six EP and three $p53^{-/-}$ lymphomas. Representative ideograms are shown in Figure 7A, with the rest presented in Figures S2 and S3 and Table S1. Whole chromosome gains of 4, 14, and 15 were common in both types of lymphomas, suggesting that P53 deficiency may nonrandomly lead to the duplication of these chromosomes. Lymphoma line EP175, which harbored a 14:5 translocation (Table 1), exhibited a mosaic (partial) gain of the chromosome 14 but not chromosome 5. Lymphoma lines with chromosome 12 translocations (EP116, EP173, and EP70) did not exhibit amplification of chromosome 12, suggesting that the translocations are not associated with amplifications.

Chromosome 9 alterations were seen in all six independently derived EP lymphoma lines (Figure 7B, Figure S2, and Table S1). While whole chromosome gain (EP173) and a partial loss (EP175) were noted, the most frequent alteration involved mosaic gains of various parts of the 9A1–A5.3 region (EP116, EP175, EP23, EP70, and EP88). Lymphoma line EP70 harbored a single amplicon, encompassing up to a 550 kb region that includes the *Ets-1* locus (Figure 7B). Southern blotting analysis confirmed that the *Ets-1* is amplified (data not shown). Other EP lymphoma lines harbored much larger amplicons (on the order of megabases), with breakpoints at various locations within the 9A1–A5.3 region. Notably, amplification breakpoints often fell near genes commonly involved in lymphoma pathogenesis in mice and humans, including *Ets-1* (EP70, EP88, EP116) (Oikawa and Yamada, 2003), *Mll* (EP23, EP88, EP175) (Greaves and Wiemels, 2003; Tanaka et al., 2001), and *Atm* (EP88, EP116) (Stilgenbauer et al., 1997).

Furthermore, we investigated the nature of mosaic amplification of chromosome 9 by SKY analysis using a chromosome 9-specific paint. As shown in Figure 6B, lymphoma line EPD1 had two normal copies of chromosome 9 as well as a tricentric chromosome 9 with amplifications. Interestingly, a fragment of chromosome 9 was visible in one SKY image, suggesting that chromosome 9 is prone to breakage. Together, these findings suggest that recurrent chromosome 9 alterations are RAG dependent and may be a significant contributing factor to the accelerated lymphomagenesis in EP mice.

RAG2 is required for the accelerated lymphomagenesis in $E\beta^{R/R}$ $p53^{-/-}$ mice

To further determine the requirement of RAG activity in the accelerated lymphoma development in EP mice, we monitored lymphoma-free survival of $E\beta^{R/R}$ $p53^{-/-}$ $RAG2^{-/-}$ (EPR) mice. Five out of 18 EPR mice died before 7 weeks of age, including one with teratocarcinoma, one with B cell lymphoma, and three with unknown cause. The rest of EPR mice succumbed to thymic lymphomas between 11 to 23 weeks of age with an average survival of 18 weeks (Figure 2A). Compared to EP mice, on average, EPR mice lived significantly longer ($p < 0.0001$), however, they still succumbed to thymic lymphoma at younger ages than $p53^{-/-}$ mice ($p = 0.0063$). Nevertheless, EPR lymphomas did not exhibit the distinct chromosomal alterations characteristic of EP lymphomas, but rather resembled $p53^{-/-}$ lymphomas in karyotypes (Figure 6 and Table 1). Together, these findings suggest that RAG activity is a critical contributing factor to the accelerated lymphomagenesis in EP mice.

Discussion

RAG activity synergizes with deficient DNA damage responses in lymphomagenesis

In this report, we present several lines of evidence to support a model in which stalled thymocyte development as an indirect consequence of Eβ inactivation results in RAG expression and inappropriate DNA cleavages that synergize with a defective DNA damage response to provoke lymphomagenesis. First, thymocyte development in the $E\beta^{R/R}$ mice is blocked at stages that normally express RAG and are prone to apoptosis. Second,

Table 1. Summary of SKY analyses

Cell lines	Genotype	Metaphase examined	Range (average)	Translocations	Frequency
EP70	$E\beta^{R/R}$ $p53^{-/-}$	18	41–62 (55)	t(12;2)	4/18
				t(12;9)	5/18
				t(1;12)	1/18
				t(9;14)	1/18
				t(9;5)	1/18
EP90	$E\beta^{R/R}$ $p53^{-/-}$	6	73–92 (88)	t(12;14) reciprocal	3/6
				t(4;18)	1/6
				t(14;2)	1/6
				t(4;8)	1/6
EP116	$E\beta^{R/R}$ $p53^{-/-}$	9	46–51 (50)	t(2;10) reciprocal	2/9
				t(12;9)	2/9
				t(12;1)	2/9
				t(9;6)	1/9
				t(14;9)	1/9
				t(18;9)	1/9
				Rb(9;5)	1/9
EP173	$E\beta^{R/R}$ $p53^{-/-}$	20	43–92 (57)	t(12;16)	20/20
EP175	$E\beta^{R/R}$ $p53^{-/-}$	16	46–64 (56)	t(14;5) reciprocal	2/16
				t(6;16)	1/16
				t(5;9)	1/6
EPD1	$E\beta^{R/R}$ $p53^{-/-}$ $TCR\delta^{-/-}$	14	42–47 (45)	t(9:9:9)	3/14
				t(9:X)	3/14
EPD16	$E\beta^{R/R}$ $p53^{-/-}$ $TCR\delta^{-/-}$	6	42–50 (46)	t(4:16)	3/6
				t(3;14)	1/6
				t(9;10)	1/6
EPD112	$E\beta^{R/R}$ $p53^{-/-}$ $TCR\delta^{-/-}$	6	40–43 (41)	t(9;16)	5/6
P99	$p53^{-/-}$	10	40–49 (45)	t(15;16)	1/10
				t(1;11)	1/10
				t(X;8)	1/10
P101	$p53^{-/-}$	11	41–57 (54)	Rb(16;2)	2/11
				Rb(16;5)	3/11
				t(6;12;6)	3/11
				t(8;12)	1/11
				t(5;8)	1/11
				t(16;14)	1/11
				t(3;16)	1/11
*	$p53^{-/-}$	5	48–50 (49)	none	
*	$p53^{-/-}$	10	39–60 (42)	t(15;15)	8/10
*	$p53^{-/-}$	10	39 (39)	t(2;19)	5/10
EPR2	$E\beta^{R/R}$ $p53^{-/-}$ $RAG2^{-/-}$	11	37–51 (44)	none	
EPR51	$E\beta^{R/R}$ $p53^{-/-}$ $RAG2^{-/-}$	11	46–52 (49)	t(10;11) reciprocal	8/11
EPR68	$E\beta^{R/R}$ $p53^{-/-}$ $RAG2^{-/-}$	10	38–49 (43)	none	

Various lymphomas were analyzed by SKY. Shown are numbers of metaphases examined and average numbers of chromosomes, as well as the range for each lymphoma line, chromosome translocations, and chromosome frequencies. t, translocation (the chromosome donating the centromere is listed first); Rb, Robertsonian translocation. *Data are from study by Liao et al. (1998).

inactivation of *P53* in the $E\beta^{R/R}$ mice resulted in a partial rescue of thymocytes from apoptosis and accelerated onset of fatal thymic lymphoma as compared to $p53^{-/-}$ mice. Third, RAG2 protein was detected during lymphomagenesis, and RAG2 transcript was detected in the resultant lymphoma lines. Fourth, Southern blotting and PCR analyses revealed RAG-mediated rearrangements at *TCR*α, *IgH*, and *Bcl11b* loci in EP lymphomas, suggesting RAG cleavages in these regions at some point in the life of the transformed clones. Fifth, most EP lymphomas harbor translocations that frequently involve chromosomes 12 or 14, which possess RAG target sites across the resident *IgH* and *TCR*α loci, respectively. These translocations are RAG dependent, as they were absent in lymphomas from EPR mice. Finally, genetic deletion of RAG2 allowed EP mice to survive an average of 18 weeks compared to 14 weeks when RAG2 is present, although the average survival of $p53^{-/-}$ mice was still longer (22 weeks). The lack of complete rescue could be due to other effects of the Eβ mutation, including difference in thymocyte development or frequency of precursor tumor cells between $p53^{-/-}$ mice and EPR mice (see below). Together, these findings implicate RAG activity as an important factor in synergizing with P53 deficiency in lymphomagenesis.

Our findings suggest a general model in which any condition that allows RAG expression would accelerate tumorigenesis in a DNA damage checkpoint-deficient background. This model is consistent with previous findings implicating inappropriate RAG-mediated DSBs at antigen receptor loci and other cryptic RSS sites throughout the genome in lymphomagenesis (Lewis et al., 1997; Marculescu et al., 2002; Raghavan et al., 2004; Sakata et al., 2004). Importantly, our findings extend the range of molecular aberrations that can drive the development of lymphomas. During lymphocyte development, RAG expression is activated at distinct developmental stages and is shut off by feedback inhibition of the functionally assembled gene products. Many mutations block lymphocyte development at a stage where RAG is naturally expressed. For example, mutations of

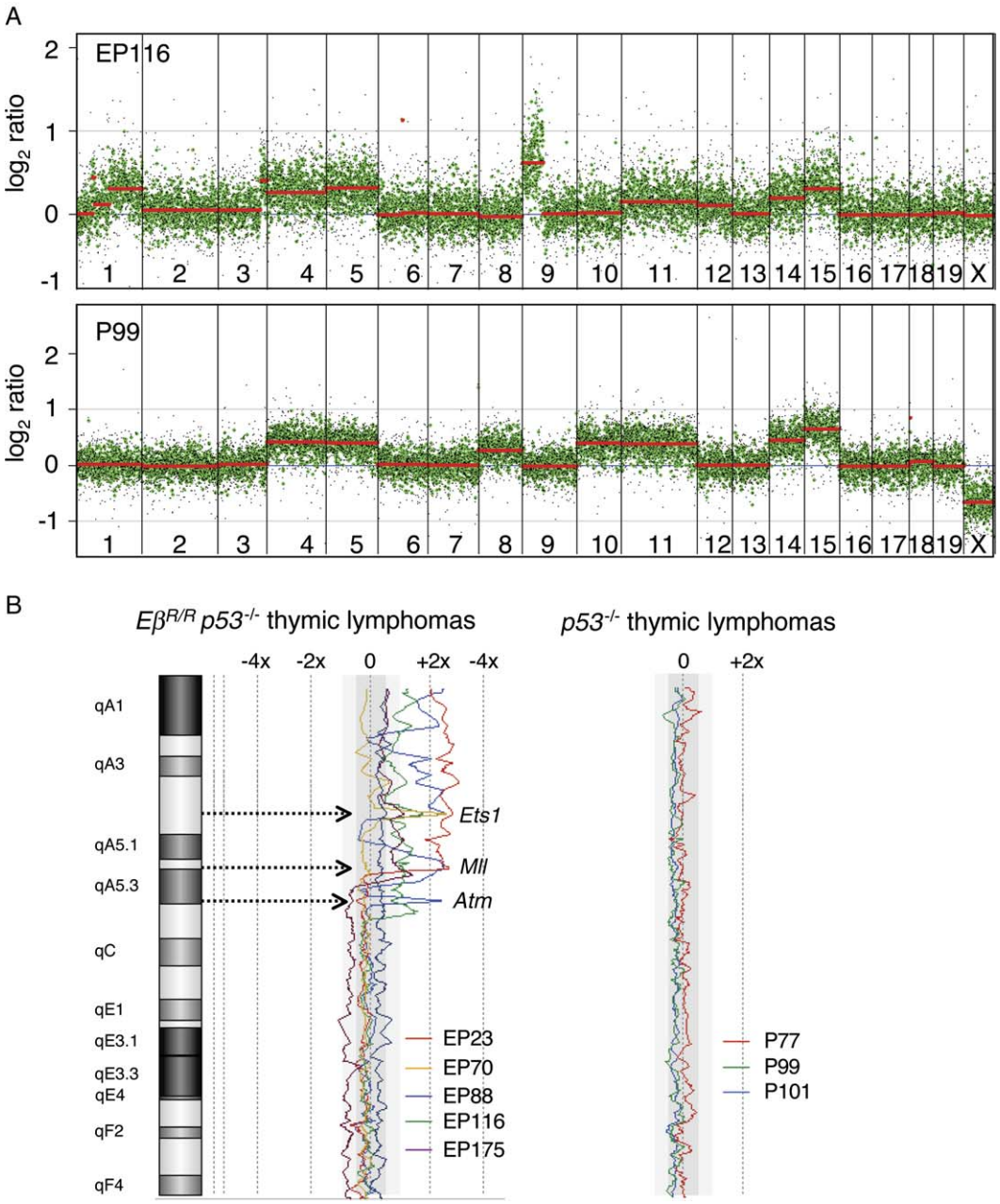

Figure 7. Array CGH analyses of $p53^{-/-}$ and $E\beta^{R/R}$ $p53^{-/-}$ lymphomas

A: Representative ideograms of one EP lymphoma (EP116) and one $p53^{-/-}$ lymphoma (P99). Chromosomes are listed in numerical order from left to right. Points above zero on y axis represent amplifications, and those below zero indicate deletions relative to the diploid control. The red line running through the individual points represents the average values. X chromosome profiles should be discounted, as some lymphomas were derived from male mice and the reference DNA was from a wild-type female mouse.

B: Overlay of chromosome 9A1–A5.3 region and array CGH signal of the indicated EP lymphomas and $p53^{-/-}$ lymphomas. Arrows indicate amplification of regions corresponding to *Ets-1*, *Mll*, and *Atm* loci.

TCRβ, *CD3ϵ*, or NHEJ genes all interfere with pre-TCR expression and therefore block T cell development at the DN3 stage where RAG is expressed. According to our model, all these mutations would be expected to accelerate development of thymic lymphomas in $p53^{-/-}$ mice. Consistent with this notion, $p53^{-/-}$ *NHEJ*$^{-}$ mice rapidly develop fatal pro-B cell lymphomas due to oncogenic translocations involving *IgH* and c-*myc* (Bassing et al., 2002).

Contribution of the $E\beta^{R/R}$ mutation to lymphomagenesis by RAG-independent mechanisms

It should be noted that the $E\beta^{R/R}$ mutation might also contribute to lymphomagenesis through mechanisms independent of its effect on RAG activity. Consistent with this notion, *RAG2* deficiency did not completely extend the lymphoma-free survival time of EP mice to that observed for $p53^{-/-}$ mice. Loss of the $E\beta$ function and consequently the inability to express pre-TCR

or TCR severely perturbs thymocyte differentiation, proliferation, and survival that can in several ways predispose to transformation. First, the DN3 stage at which most $E\beta^{R/R}$ thymocytes are blocked has been shown to exhibit heightened kinase activity, lower signaling thresholds, and proclivity to transformation (Haks et al., 2003). Second, DN to DP progression in $p53^{-/-}$ mice without proper pre-TCR signaling can lead to cellular transformation (Haks et al., 1999), even in the absence of *RAG* (Jiang et al., 1996). Consistently, we found that lymphomagenesis in EP mice requires DN to DP progression, and the transition is RAG independent. Third, $E\beta^{R/R}$ thymocytes exhibit significantly elevated levels of apoptosis relative to wild-type or $p53^{-/-}$ thymocytes, and only a portion of this apoptosis is prevented by the loss of P53, indicating that $E\beta^{R/R}$ thymocytes experience other stresses that may cooperate with the P53 deficiency in lymphomagenesis. Nevertheless, given that the lymphomas in EP, EPR, and EPD mice all exhibit $CD4^+CD8^+$ or $CD8^+$ phenotypes, the precise role of arrested T cell development in the observed lymphomagenesis remains to be determined.

Characteristic chromosome translocations and amplifications in accelerated lymphomagenesis of EP mice

We found frequent *IgH* and *TCRα* rearrangements, and correspondingly chromosome 12 and 14 translocations, in EP thymic lymphomas. The most frequent chromosomal alterations in EP lymphomas are mosaic gains of the 9A1–A5.3 region. We also noted frequent involvement of chromosome 9 in translocations with chromosomes 12 or 14 as well as with itself (tricentric). Alterations of the 9A1–A5.3 region are also frequently observed in $H2AX^{-/-}$ $p53^{-/-}$ thymic lymphomas (Celeste et al., 2003) and $p53^{-/-}$ $NHEJ^-$ pro-B lymphomas (Zhu et al., 2002). Several genes known to be involved in DNA damage responses and genome integrity, such as *Atm* (Stilgenbauer et al., 1997) and *H2AX* (Bassing et al., 2003; Celeste et al., 2003), and oncogenesis, such as *Mll* (Greaves and Wiemels, 2003; Tanaka et al., 2001) and *Ets-1* (Oikawa and Yamada, 2003), are located within this region and fall within amplification breakpoint regions in EP lymphomas. Notably, the syntenic 11q22–25 region in humans is also frequently deleted, rearranged, or amplified in many hematological malignancies (Greaves and Wiemels, 2003) and is associated with a worsened prognosis (Monni and Knuutila, 2001). Similarly, translocations involving the *IgH* and *TCRα* loci are frequently found in human lymphomas and leukemias (Tycko and Sklar, 1990; Vanasse et al., 1999). It is likely that RAG-induced alterations to the chromosome region 9A1–A5.3 or chromosome 12 and 14 translocations provide a selective advantage to emergent EP clones, either through oncogene activation or inactivation of genes required for genome stability and DNA repair.

Studies in mice deficient in both P53 and NHEJ have identified *IgH*/c-*myc* translocation involving a complex B-F-B mechanism as the critical event for the development of pro-B cell lymphomas (Zhu et al., 2002). Although we observed chromosome 9 fragmentation and tricentric formation, we did not frequently observe the B-F-B intermediates or products. This is probably because most of RAG-mediated cleavages are repaired in EP thymocytes, whereas in $p53^{-/-}$ $NHEJ^-$ mice, breaks generated during V(D)J recombination cannot be repaired by the NHEJ pathway but have to exert alternative, error-prone microhomology-directed repair that could initiate the B-F-B cycle. Consistently, P53 activation was observed in primary lymphoid organs of $NHEJ^-$ mice (Danska et al., 1996), but not in wild-type or $E\beta^{R/R}$ mice (data not shown). The differences underscore the distinctions in lymphomagenesis between the EP model and $p53^{-/-}$ $NHEJ^-$ model.

Cellular pathways of thymic lymphomagenesis

One of the striking feature of lymphomagenesis in EP, EPD, and EPR mice is that tumor cells were DP or CD8 SP and that the emergence of these tumor cell populations was preceded by the development of DP cells. As normal thymocyte development progresses from DN to DP and then to SP stages, these findings raise the question as to whether the normal development pathway is coopted by lymphomagenesis in the mutant mice. While the preexistence of DP cells in EP mice allows the possibility that lymphomagenesis occurs within this cell population, this cannot be the case for EPD or EPR mice, whose thymus is initially composed solely of DN cells. Further supporting this hypothesis, introduction of $p53^{-/-}$ mutation into $RAG2^{-/-}$ or $CD3\gamma^{-/-}$ mice promotes DN to DP thymocyte differentiation before the development of DP or CD8 SP thymic lymphomas (Haks et al., 1999; Jiang et al., 1996; Nacht and Jacks, 1998). Enforced DN to DP progression by introduction of a *TCR* transgene in $p53^{-/-}$ $RAG1^{-/-}$ mice also accelerates development of thymic lymphomas (Liao et al., 1998). One of the key events that occur during DN to DP differentiation is cell proliferation. It is possible that this proliferation is also required for the outgrowth of transformed clones. Whether transformation takes place in DN cells, which then differentiate into DP stages, or whether the process of DN to DP transition is involved in the transformation events remains to be determined.

Experimental procedures

Mice and genotyping

$E\beta^{R/R}$ $p53^{-/-}$ mice were generated by mating $E\beta^{R/R}$ with $p53^{-/-}$, followed by mating of F1 heterozygous siblings. Due to their rapid development of thymic lymphoma, EP mice were maintained and generated by $E\beta^{R/R}$ $p53^{+/-}$ matings. To generate $E\beta^{R/R}$ $p53^{-/-}$ $TCR\delta^{-/-}$ mutants, $TCR\delta^{-/-}$ mice (Jackson Laboratory, Bar Harbor, ME) were crossed to $E\beta^{R/R}$ $p53^{+/-}$ mice. The Eβ and TCRδ mutant alleles were bred to homozygosity, while p53 alleles were maintained in a heterozygous state for matings. $E\beta^{R/R}$ $p53^{-/-}$ $RAG2^{-/-}$ mice were generated and maintained by mating $E\beta^{R/R}$ $p53^{+/-}$ to $RAG2^{-/-}$ mice. Genotyping of $E\beta^{R/R}$ and $p53^{-/-}$ was performed by PCR of genomic tail DNA (Jacks et al., 1994; Ryu et al., 2003). Genotyping of $TCR\delta^{-/-}$ mice was done following protocols provided by the Jackson Laboratory. The primers for RAG2 genotyping were 5′-TCTCCAGAACTTCAG GATG and 5′-AGCCTGCTTATTGTCTCCTG for wild-type allele, and 5′-AGCCTGCTTATTGTCTCCTG and 5′-GGCACCGGACAGGTCGGTCTTGAC for mutant allele. All experiments with mice were performed in accordance with the regulations of the MIT Committee on Animal Care (Protocol 0304-021-07).

Flow cytometry

Thymocytes (1–10 × 10^6) were suspended in FACS buffer (0.1% FCS plus 0.02% sodium azide) and incubated with the indicated antibodies on ice for 30 min, followed by two washes. Data were collected on a FACSCalibur (Becton Dickinson) and analyzed with CellQuest software. All antibodies were purchased from Pharmingen (San Diego, CA). For analysis of apoptosis, thymocytes were first incubated with a cocktail of CD4-APC, CD8-Cy5.5, and TCRγδ-PE antibodies. The cells were then resuspended in 100 μl annexin binding buffer (10 mM HEPES/NaOH [pH 7.4], 140 mM NaCl, 2.4 mM CaCl) supplemented with 5 μl of annexin IV-FITC and 2.5 μl of 100 μg/ml DAPI (Pierce). A total of 1–1.5 × 10^6 events were collected on a MoFlo3

(Cytomation), and the data were analyzed using Summit software. For cell cycle analyses, thymocytes were stained with FITC-conjugated CD4 and CD8 and then permeabilized with Saponin buffer (0.1% Saponin, 1% BSA, 0.02% sodium azide in PBS). The cell pellet was resuspended in Saponin buffer containing 200 μg/ml PI and 50 μg/ml RNaseA (Sigma), followed by incubation at 15 min at 4ºC.

Southern and Northern blotting and PCR

Genomic DNA isolation and Southern blotting were performed as described (Ryu et al., 2003). The Jα49-48 intron probe was amplified by PCR with primers 5′-GTAAGTGTGAGGCTATCTAACC and 5′-CATTAGTAAGCACT TATTTCAGG. Dβ1–Jβ1, Dβ2–Jβ2, and Cβ1 probes were as described (Whitehurst et al., 1999). All probes were labeled by random priming with ^{32}P-dCTP. For Northern analysis, 10 μg of total RNA was fractionated on a 1% formaldehyde agarose gel and transferred to Zeta-probe membrane (Bio-Rad). The membrane was sequentially hybridized with ^{32}P-labeled RAG2 and GAPDH cDNA probes. Standard nested PCR to amplify internal *Bcl11b* deletions was performed as described (Sakata et al., 2004). All PCR products were cloned, and five clones originating from each cell line were sequenced. Digestion-circularization PCR was used to clone the Eμ-hybridizing J_H fragments from thymic lymphomas. Genomic DNA was digested with EcoRI, diluted, and ligated. Circularized DNA was then used as template for the primary PCR amplification using the primers 5′-TTGAGCAATGTT GAGTTGAGTC and 5′-CTGAATAGGGTATGAGAGAGAGCCT. Then, 5 μl of the primary PCR mixture was subjected to the secondary PCR using the primers 5′-GATGGCCGATCAGAACCGGAACA and 5′-CCCATTCCTCGGT TAAACTTTAAG. PCR products were cloned and sequenced.

SKY and array CGH

Metaphase chromosomes were prepared from thymic lymphoma lines at early passage numbers (1–3). Cells were incubated in 0.1 mg/ml Colcemid for 30–60 min and then incubated in 75 mM KCl. Chromosomes were subsequently fixed in 3:1 methanol:acetic acid and dropped onto glass slides. Metaphase spreads were incubated with mouse SkyPaint kit probe (Applied Spectral Imaging, Carlsbad, CA) followed by counterstain with DAPI. Raw spectral images were visualized by assigning red, green, and blue colors to specific spectral ranges. Chromosomes were identified using SKY View software (Applied Spectral Imaging). Chromosome aberrations were defined using the nomenclature rules from the Committee on Standard Genetic Nomenclature for Mice. Six to twenty metaphases were analyzed for each lymphoma line. Statistical analysis was performed by χ^2 test, and p value was determined by Monte Carlo simulation with 10^7 random iterations. For array CGH analyses, DpnII-digested genomic DNA from primary $E\beta^{R/R}$ $p53^{-/-}$ or $p53^{-/-}$ thymic lymphomas were used for labeling reactions and hybridized to the Mouse Development Oligo Microarray (G4121A, Agilent Technologies, Palo Alto, CA). Wild-type thymus genomic DNA was used as control. Data were assembled and analyzed using CGH Analytics software (Agilent Technologies).

Supplemental data

The Supplemental Data include three supplemental figures and one supplemental table and can be found with this article online at http://www.cancercell.org/cgi/content/full/9/2/109/DC1/.

Acknowledgments

We thank Dr. Tyler Jacks for $p53^{-/-}$ mice, Drs. Herman N. Eisen and Tania Baker for manuscript review, and members of the Chen laboratory for helpful discussions. This work was supported in part by grants AI40416 and CA100875 from the National Institutes of Health and David Koch Research Fund (to J.C.), a Cancer Center Core Grant (to Tyler Jacks), a grant from Korea Science and Engineering Foundation (R01-2004-000-10047-0 to C.J.R.), and a grant from the Nano-Bio Research and Development Program of the Ministry of Science and Technology, Korea (TNM0200512 to H.J.H.). S.C. is supported by the Ellison Medical Foundation, NIH grant AG01019, and a Belfer Cancer Core grant to the DFCI. R.A.D. is an American Cancer Society Research Professor and an Ellison Foundation Senior Scholar and is supported by grants from the NIH and ACS. B.B.H. was partly supported by a Postdoctoral Fellowship from the American Cancer Society (PF0122801), and A.L. was partly supported by a Research Fellowship from the Deutsche Forschungsgemeinschaft (LU 841/2-1). Array CGH profiles were performed at the Arthur and Rochelle Belfer Cancer Genomic Center at the Dana-Farber Cancer Institute.

Received: July 14, 2005
Revised: October 12, 2005
Accepted: January 9, 2006
Published: February 13, 2006

References

Bassing, C.H., Swat, W., and Alt, F.W. (2002). The mechanism and regulation of chromosomal V(D)J recombination. Cell Suppl. *109*, S45–S55.

Bassing, C.H., Suh, H., Ferguson, D.O., Chua, K.F., Manis, J., Eckersdorff, M., Gleason, M., Bronson, R., Lee, C., and Alt, F.W. (2003). Histone H2AX: A dosage-dependent suppressor of oncogenic translocations and tumors. Cell *114*, 359–370.

Bendelac, A., Matzinger, P., Seder, R.A., Paul, W.E., and Schwartz, R.H. (1992). Activation events during thymic selection. J. Exp. Med. *175*, 731–742.

Bouvier, G., Watrin, F., Naspetti, M., Verthuy, C., Naquet, P., and Ferrier, P. (1996). Deletion of the mouse T-cell receptor β gene enhancer blocks αβ T-cell development. Proc. Natl. Acad. Sci. USA *93*, 7877–7881.

Celeste, A., Difilippantonio, S., Difilippantonio, M.J., Fernandez-Capetillo, O., Pilch, D.R., Sedelnikova, O.A., Eckhaus, M., Ried, T., Bonner, W.M., and Nussenzweig, A. (2003). H2AX haploinsufficiency modifies genomic stability and tumor susceptibility. Cell *114*, 371–383.

Chu, G. (1997). Double strand break repair. J. Biol. Chem. *272*, 24097–24100.

Danska, J.S., Holland, D.P., Mariathasan, S., Williams, K.M., and Guidos, C.J. (1996). Biochemical and genetic defects in the DNA-dependent protein kinase in murine scid lymphocytes. Mol. Cell. Biol. *16*, 5507–5517.

Difilippantonio, M.J., Zhu, J., Chen, H.T., Meffre, E., Nussenzweig, M.C., Max, E.E., Ried, T., and Nussenzweig, A. (2000). DNA repair protein Ku80 suppresses chromosomal aberrations and malignant transformation. Nature *404*, 510–514.

Difilippantonio, M.J., Petersen, S., Chen, H.T., Johnson, R., Jasin, M., Kanaar, R., Ried, T., and Nussenzweig, A. (2002). Evidence for replicative repair of DNA double-strand breaks leading to oncogenic translocation and gene amplification. J. Exp. Med. *196*, 469–480.

Dudley, E.C., Petrie, H.T., Shah, L.M., Owen, M.J., and Hayday, A.C. (1994). T cell receptor β chain gene rearrangement and selection during thymocyte development in adult mice. Immunity *1*, 83–93.

Engel, I., and Murre, C. (2002). Disruption of pre-TCR expression accelerates lymphomagenesis in E2A-deficient mice. Proc. Natl. Acad. Sci. USA *99*, 11322–11327.

Frank, K.M., Sharpless, N.E., Gao, Y., Sekiguchi, J.M., Ferguson, D.O., Zhu, C., Manis, J.P., Horner, J., DePinho, R.A., and Alt, F.W. (2000). DNA ligase IV deficiency in mice leads to defective neurogenesis and embryonic lethality via the p53 pathway. Mol. Cell *5*, 993–1002.

Fugmann, S.D., Lee, A.I., Shockett, P.E., Villey, I.J., and Schatz, D.G. (2000). The RAG proteins and V(D)J recombination: complexes, ends, and transposition. Annu. Rev. Immunol. *18*, 495–527.

Gao, Y., Ferguson, D.O., Xie, W., Manis, J.P., Sekiguchi, J., Frank, K.M., Chaudhuri, J., Horner, J., DePinho, R.A., and Alt, F.W. (2000). Interplay of p53 and DNA-repair protein XRCC4 in tumorigenesis, genomic stability and development. Nature *404*, 897–900.

Gladdy, R.A., Taylor, M.D., Williams, C.J., Grandal, I., Karaskova, J., Squire, J.A., Rutka, J.T., Guidos, C.J., and Danska, J.S. (2003). The RAG-1/2 endonuclease causes genomic instability and controls CNS complications of lymphoblastic leukemia in p53/Prkdc-deficient mice. Cancer Cell *3*, 37–50.

Godfrey, D.I., Kennedy, J., Mombaerts, P., Tonegawa, S., and Zlotnik, A. (1994). Onset of TCR-β gene rearrangement and role of TCR-β expression during $CD3^-CD4^-CD8^-$ thymocyte differentiation. J. Immunol. *152*, 4783–4792.

Greaves, M.F., and Wiemels, J. (2003). Origins of chromosome translocations in childhood leukaemia. Nat. Rev. Cancer *3*, 639–649.

Gu, Y., Seidl, K.J., Rathbun, G.A., Zhu, C., Manis, J.P., van der Stoep, N., Davidson, L., Cheng, H.L., Sekiguchi, J.M., Frank, K., et al. (1997). Growth retardation and leaky SCID phenotype of Ku70-deficient mice. Immunity *7*, 653–665.

Guidos, C.J., Williams, C.J., Grandal, I., Knowles, G., Huang, M.T.F., and Danska, J.S. (1996). V(D)J recombination activates a p53-dependent DNA damage checkpoint in *scid* lymphocyte precursors. Genes Dev. *10*, 2038–2054.

Haks, M.C., Krimpenfort, P., van den Brakel, J.H., and Kruisbeek, A.M. (1999). Pre-TCR signaling and inactivation of p53 induces crucial cell survival pathways in pre-T cells. Immunity *11*, 91–101.

Haks, M.C., Belkowski, S.M., Ciofani, M., Rhodes, M., Lefebvre, J.M., Trop, S., Hugo, P., Zuniga-Pflucker, J.C., and Wiest, D.L. (2003). Low activation threshold as a mechanism for ligand-independent signaling in pre-T cells. J. Immunol. *170*, 2853–2861.

Jacks, T., Remington, L., Williams, B.O., Schmitt, E.M., Halachmi, S., Bronson, R.T., and Weinberg, R.A. (1994). Tumor spectrum analysis in p53-mutant mice. Curr. Biol *4*, 1–7.

Jhappan, C., Morsle, H.C., III, Fleischmann, R.D., Gottesman, M.M., and Merlino, G. (1997). DNA-PKcs: a T-cell tumour suppressor encoded at the mouse scid locus. Nat. Genet. *17*, 483–486.

Jiang, D., Lenardo, M.J., and Zuniga-Pflucker, J.C. (1996). p53 prevents maturation to the CD4+CD8+ stage of thymocyte differentiation in the absence of T cell receptor rearrangement. J. Exp. Med. *183*, 1923–1928.

Khanna, K.K., and Jackson, S.P. (2001). DNA double-strand breaks: signaling, repair and the cancer connection. Nat. Genet. *27*, 247–254.

Leduc, I., Hempel, W.M., Mathieu, N., Verthuy, C., Bouvier, G., Watrin, F., and Ferrier, P. (2000). T cell development in TCRβ enhancer-deleted mice: implications for αβ T cell lineage commitment and differentiation. J. Immunol. *165*, 1364–1373.

Lee, G.S., Neiditch, M.B., Salus, S.S., and Roth, D.B. (2004). RAG proteins shepherd double-strand breaks to a specific pathway, suppressing error-prone repair, but RAG nicking initiates homologous recombination. Cell *117*, 171–184.

Levelt, C.N., and Eichmann, K. (1995). Receptors and signals in early thymic selection. Immunity *3*, 667–672.

Lewis, S.M., Agard, E., Suh, S., and Czyzyk, L. (1997). Cryptic signals and the fidelity of V(D)J joining. Mol. Cell. Biol. *17*, 3125–3136.

Li, G.C., Ouyang, H., Li, X., Nagasawa, H., Little, J.B., Chen, D.J., Ling, C.C., Fuks, Z., and Cordon-Cardo, C. (1998). Ku70: A candidate tumor suppressor gene for murine T cell lymphoma. Mol. Cell *2*, 1–8.

Liao, M.J., Zhang, X.X., Hill, R., Gao, J., Qumsiyeh, M.B., Nichols, W., and Van Dyke, T. (1998). No requirement for V(D)J recombination in p53-deficient thymic lymphoma. Mol. Cell. Biol. *18*, 3495–3501.

Marculescu, R., Le, T., Simon, P., Jaeger, U., and Nadel, B. (2002). V(D)J-mediated translocations in lymphoid neoplasms: a functional assessment of genomic instability by cryptic sites. J. Exp. Med. *195*, 85–98.

Mathieu, N., Hempel, W.M., Spicuglia, S., Verthuy, C., and Ferrier, P. (2000). Chromatin remodeling by the T cell receptor (TCR)-β gene enhancer during early T cell development: Implications for the control of TCR-β locus recombination. J. Exp. Med. *192*, 625–636.

McBlane, J.F., van Gent, D.C., Ramsden, D.A., Romeo, C., Cuomo, C.A., Gellert, M., and Oettinger, M.A. (1995). Cleavage at a V(D)J recombination signal requires only RAG1 and RAG2 proteins and occurs in two steps. Cell *83*, 387–395.

Monni, O., and Knuutila, S. (2001). 11q deletions in hematological malignancies. Leuk. Lymphoma *40*, 259–266.

Monroe, R.J., Seidl, K.J., Gaertner, F., Han, S., Chen, F., Sekiguchi, J., Wang, J., Ferrini, R., Davidson, L., Kelsoe, G., and Alt, F.W. (1999). RAG2:GFP knockin mice reveal novel aspects of RAG2 expression in primary and peripheral lymphoid tissues. Immunity *11*, 201–212.

Nacht, M., and Jacks, T. (1998). V(D)J recombination is not required for the development of lymphoma in p53-deficient mice. Cell Growth Differ. *9*, 131–138.

Nacht, M., Strasser, A., Chan, Y.R., Harris, A.W., Schlissel, M., Bronson, R.T., and Jacks, T. (1996). Mutations in the p53 and SCID genes cooperate in tumorigenesis. Genes Dev. *10*, 2055–2066.

Oikawa, T., and Yamada, T. (2003). Molecular biology of the Ets family of transcription factors. Gene *303*, 11–34.

Raghavan, S.C., Swanson, P.C., Wu, X., Hsieh, C.L., and Lieber, M.R. (2004). A non-B-DNA structure at the Bcl-2 major breakpoint region is cleaved by the RAG complex. Nature *428*, 88–93.

Roth, D.B., Menetski, J.P., Nakajima, P.B., Bosma, M.J., and Gellert, M. (1992). V(D)J recombination: Broken DNA molecules with covalently sealed (Hairpin) coding ends in scid mouse thymocytes. Cell *70*, 983–991.

Rothenberg, E.V., and Taghon, T. (2005). Molecular genetics of T cell development. Annu. Rev. Immunol. *23*, 601–649.

Ryu, C.J., Haines, B.B., Draganov, D.D., Kang, Y.H., Whitehurst, C.E., Schmidt, T., Hog, H.J., and Chen, J. (2003). The T cell receptor β enhancer promotes access and pairing of Dβ and Jβ gene segments during V(D)J recombination. Proc. Natl. Acad. Sci. USA *100*, 13465–13470.

Sakata, J., Inoue, J., Ohi, H., Kosugi-Okano, H., Mishima, Y., Hatakeyama, K., Niwa, O., and Kominami, R. (2004). Involvement of V(D)J recombinase in the generation of intragenic deletions in the Rit1/Bcl11b tumor suppressor gene in γ-ray-induced thymic lymphomas and in normal thymus of the mouse. Carcinogenesis *25*, 1069–1075.

Schlissel, M., Constantinescu, A., Morrow, T., Baxter, M., and Peng, A. (1993). Double-strand signal sequence breaks in V(D)J recombination are blunt, 5′-phosphorylated, RAG-dependent and cell cycle regulated. Genes Dev. *7*, 2520–2532.

Stilgenbauer, S., Schaffner, C., Litterst, A., Liebisch, P., Gilad, S., Bar-Shira, A., James, M.R., Lichter, P., and Dohner, H. (1997). Biallelic mutations in the ATM gene in T-prolymphocytic leukemia. Nat. Med. *3*, 1155–1159.

Tanaka, K., Eguchi, M., Eguchi-Ishimae, M., Hasegawa, A., Ohgami, A., Kikuchi, M., Kyo, T., Asaoku, H., Dohy, H., and Kamada, N. (2001). Restricted chromosome breakpoint sites on 11q22-q23.1 and 11q25 in various hematological malignancies without MLL/ALL-1 gene rearrangement. Cancer Genet. Cytogenet. *124*, 27–35.

Tycko, B., and Sklar, J. (1990). Chromosomal translocations in lymphoid neoplasia: A reappraisal of the recombinase model. Cancer Cells *2*, 1–8.

Vanasse, G.J., Concannon, P., and Willerford, D.M. (1999). Regulated genomic instability and neoplasia in the lymphoid lineage. Blood *94*, 3997–4010.

van Gent, D.C., Hoeijmakers, J.H., and Kanaar, R. (2001). Chromosomal stability and the DNA double-stranded break connection. Nat. Rev. Genet. *2*, 196–206.

Whitehurst, C., Chattopadhyay, S., and Chen, J. (1999). Control of V(D)J recombinational accessibility of the Dβ1 gene segment at the TCRβ locus by a germline promoter. Immunity *10*, 313–322.

Zhu, C., Mills, K.D., Ferguson, D.O., Lee, C., Manis, J., Fleming, J., Gao, Y., Morton, C.C., and Alt, F.W. (2002). Unrepaired DNA breaks in p53-deficient cells lead to oncogenic gene amplification subsequent to translocations. Cell *109*, 811–821.